CEES 2020
12 — 15 OCTOBER 2021
COIMBRA | PORTUGAL
INTERNATIONAL CONFERENCE
CONSTRUCTION, ENERGY
ENVIRONMENT & SUSTAINABILITY

CHARACTERIZATION OF THERMAL ENERGY DYNAMICS OF MULTI-ZONE RESIDENTIAL BUILDINGS AFTER PRE-COOLING

Shayan Naderi [1,2,3]
Gloria Pignatta [1,2]
Iain MacGill [3,4]
Simon Heslop [3,5]
Dong Chen [6]

[1] School of Built Environment, University of New South Wales (UNSW), Sydney | Australia
[2] High Performance Architecture Research Cluster, University of New South Wales (UNSW), Sydney | Australia
[3] Centre for Energy & Environmental Markets, University of New South Wales (UNSW), Sydney | Australia
[4] School of Electrical Engineering and Telecommunications, University of New South Wales (UNSW), Sydney | Australia
[5] School of Photovoltaics and Renewable Energy Engineering, University of New South Wales (UNSW), Sydney | Australia
[6] The Commonwealth Scientific and Industrial Research Organisation (CSIRO), Melbourne | Australia
Corresponding author: g.pignatta@unsw.edu.au

Keywords
Building Energy Efficiency, Thermal Mass, Demand Side Management, Cooling Decay, Time Constant, Thermal Capacitance

Abstract
The energy consumption of air conditioners for residential cooling applications creates a peak electricity demand in the afternoon. This increases households' electricity bills because the electricity tariff rates are expensive during peak hours. One practical solution to flatten the demand profile and shift the load to times with lower demand is pre-cooling. Pre-cooling involves running air conditioners to cool the thermal mass of buildings before peak demand. Due to the lack of insulation, and thermal mass characteristics, the energy consumed during pre-cooling events is higher than the peak load reduction, and the ratio of peak load reduction to the extra energy consumption highly depends on the thermal dynamics of the building. Therefore, pre-cooling in some houses might not be an economic choice. This necessitates the characterization of building thermal dynamics to quantify the pre-cooling potentials of buildings and conditioned zones and avoid wasting energy in leaky houses. In this paper, the temporal change in indoor and thermal mass temperature, in Australian residential buildings, is simulated using a second-order linear differential equation (SDE) system and a dataset generated by AccuRate, a tool developed by CSIRO for rating Australian buildings. The data of indoor temperature, outdoor temperature, and solar radiation between the last cooling event and midnight of each day is fed into the model. The SDE system is converted into an autoregressive model by integrating over the sampling interval. Based on the transfer function of the autoregressive model, two different time constants, one short and one long are obtained for the modelled Australian houses to characterize their thermal response after each pre-cooling event. The former describes the heat transfer between building thermal mass and indoor air while the latter describes the time for heat transfer between indoor and outdoor air. It is observed that houses/zones with a higher time constant keep coolness for longer periods, making them more suitable for pre-cooling applications. In February, building B retains thermal comfort for less than two hours after pre-cooling to 22°C while the case study with higher time constants, building M, retains thermal comfort for the next eight hours. If there is a peak in temperature evolution profile, it occurs earlier and is sharper in those buildings/zones with smaller time constants. Furthermore, if two zones have equal long-term time constants, the one with a higher short-term time constant is more suitable for pre-cooling applications. These findings highlight the reliability of time constants for ranking buildings based on their ability to maintain thermal comfort after pre-cooling.

1.1 INTRODUCTION

Looking at the data of electricity consumption of the residential sector in Australia, it emerges that there is a peak around 5:00 PM for apartment units and 5:30 PM for houses [1]. Statistics show that on average, Air Conditioning (AC) can be responsible for around 50% of the peak demand in Australian eastern capital cities [2]. The reason is that people arrive home in the afternoon and turn on the AC system to make the house comfortable. It leads to a spike in network electricity demand, and infrastructure underutilization since the capacity of the electricity network must be able to meet the peak demand, which only occurs a few hours in a year. Furthermore, when the demand increases, the network operators run power plants with higher operational costs, which results in a higher levelized cost of electricity [3]. This extra cost is passed to the households through expensive electricity rates during peak periods, resulting in high electricity bills.

There are solutions to overcome the high peak consumption that can be implemented at a low-voltage distribution network, where small commercial and residential buildings are located. One of the feasible solutions is load shifting using building thermal mass [4]. Building thermal mass includes building envelopes, structure, construction materials, and furniture. Each of these components has a thermal storage capacity and different thermal dynamics [5]. Charging and discharging the capacity of thermal mass via thermal energy is called thermal mass activation, which can be done through four different methods [6] namely surface activation, forced-air activation, hydronic activation, and electrical activation. The most common method is surface activation since it does not require any extra investment and can be done using almost all the existing AC systems. By charging the thermal mass and discharging it later, a proportion of the load associated with air conditioning can be shifted. If the discharge time is before the peak load period, and the discharge occurs during the peak period, the thermal mass activation process leads to peak load shifting.

Pre-cooling is the act of lowering the temperature of thermal mass before the peak period to store coolness and release it during peak hours [7-9]. In a pre-cooling strategy, the thermostat setpoint is reduced a few hours before the peak and it is increased while the demand and electricity rates are high. When the thermostat setpoint is high, the AC system is turned off, but the stored coolness in the thermal mass does not allow the indoor temperature to rise quickly. The thermal mass acts as a heat sink and releases the coolness at a slower rate than the indoor temperature, mainly due to the higher specific heat capacity of thermal mass compared to air [5]. Consequently, the indoor air temperature remains within the thermal comfort range for a period that is long enough to reduce AC cooling requirements during the evening peak demand period, resulting in a reduction in household electricity bills [10]. Thermal comfort, which is a function of indoor air psychrometric properties, clothing, and occupants' metabolic rate, is defined as the expression of satisfaction from the indoor thermal environment [11].

The time that the indoor environment remains thermally comfortable depends on many factors including weather condition [12], level of insulation [13, 14], quantity and quality of thermal mass [5], internal heat gains, and the type of AC (such as evaporative cooling or forced-air thermal mass activation). Also, depending on the orientation of the building and interaction between conditioned zones, each zone might have different thermal dynamics [15]. Due to the performance gap of buildings, which is the difference between design and real construction [16, 17], and also the fact that the quantity of thermal mass is hard to measure, it is not accurate to estimate the thermal performance of buildings based on the construction materials and design. Therefore, data-driven models are frequently used to understand the thermal dynamics of buildings. Decrement factor and time lag [12], building airtightness [14], long and short term time constants [18, 19], heat loss coefficient [20], and decay factor [21] are some of the metrics that have been extracted using the operational data of the building to quantify its thermal dynamics.

Based on the indoor temperature measurement of a house, Madsen and Holst [19] concluded that at least two different time constants are required to describe a buildings' thermal response. If a single heat capacitance and time constant is considered for a building, such as that proposed by Andrew Law [21], the short term variations cannot be captured. Another problem with models based on decay factor and Newton's cooling law [21] is that they are derived from the difference between indoor and outdoor temperature profiles. Therefore, different inputs such as solar radiation or wind speed cannot be fed into the model to consider their effects on decay cooling profile. To obtain two different time constants and consider more inputs, Madsen and Holst [19] proposed a model with two different heat capacitances, one for the thermal mass and one for the indoor air temperature and simulated a building in a cold climate. Palmer Real et al. [14] simulated the temperature decay of Danish buildings overnight and classified them based on their time constants. Their results highlight that the long-term time constant represents the main thermal dynamics, and lower values for this term mean that the building has a faster rate of temperature decay overnight. The abovementioned studies used time constants and the decay factor for heating applications.

To the best of the authors' knowledge, there is no unique method to quantify the pre-cooling potentials of different zones of a building based on their thermal dynamics. In this paper, we modified the method presented in [18] to calculate two different time constants for the thermal response after each cooling event in three multi-zone Australian buildings. We added solar radiation data to the model of Palmer Real et al. [18] to validate the applicability of the model to capture daytime thermal dynamics. Moreover, this is the first study investigating thermal dynamics of a multi-zone building using its time constants, and the first time that these time constants are used for cooling applications. With the help of the obtained time constants, we rank zones based on their pre-cooling potential and their ability to maintain thermal comfort after pre-cooling.

The rest of the paper is organized as follows: Methodology, section 1.2, followed by data description (section 1.3), model development (section 1.4), and parameter estimation (section 1.5). Results and discussion, section 1.6, describes the outcomes of the study followed by conclusions in section 1.7.

1.2 METHODOLOGY

In this section, the dataset and the procedure used for the calculation of time constants after pre-cooling are described. It includes data preparation, deriving an autoregressive model from a second-order stochastic differential equation (SDE), extracting the transfer function of the autoregressive model, and the least-square method for parameter estimation.

1.3 DATA AND CASE STUDIES

In this study, data for three multi-zone buildings were used. The dataset is 12 months' worth of indoor air temperature, outdoor air temperature, solar radiation and AC consumption data from CSIRO's home energy rating tool, AccuRate [22]. The energy used by AC units in each zone is controlled separately. The details of each case study are presented in Table 1.

Table 1. Details of the three case study buildings.

Name	Number of Floors	Number of Zones	Number of Conditioned Zones	Location	Climate Zone
B	1	13	8	Brisbane	Warm humid summer, mild winter
M	2	26	20	Melbourne	Mild temperate
M_2	2	20	16	Melbourne	Mild temperate

1.4 MODEL

Figure 1 shows a schematic of the interaction between building thermal mass, indoor air, and outdoor air. Building materials and furniture exchange heat with the indoor air, and then heat transfers from indoor air to outdoor air and the other way round. τ_1 and τ_2 are the time constants of these two processes, respectively.

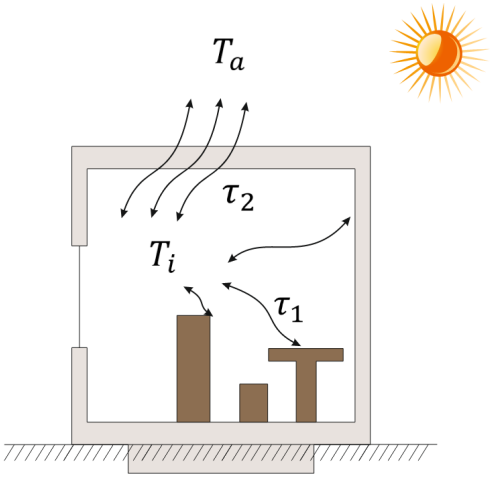

Figure 1. A schematic of the heat transfer between thermal mass, indoor air (T_i) and outdoor air (T_a).

The change of indoor and thermal mass temperatures (dT_i and dT_m) is simulated by equation (1), which is a second-order linear SDE. In this equation that describes the relationship between cooling power, physical properties, and indoor temperature evolution, T_i and T_m are indoor and thermal mass temperatures, respectively. The exogenous inputs are global solar radiation, I_g, space cooling power, Q, and outdoor temperature, T_a. Model parameters are thermal capacity of indoor air, C_i, thermal capacity of thermal mass, C_m, thermal resistance between indoor air and ambient air, R_a, thermal resistance between indoor air and thermal mass, R_i, and effective window area, A_w. The term $\sigma_k d\omega_k \forall k \in [1,2]$ is a stochastic term representing a Wiener process with variance ${\sigma_k}^2 \forall k \in [1,2]$ to account for model uncertainty.

$$\begin{cases} dT_i = \frac{1}{C_i}\left(\frac{1}{R_a}(T_a - T_i) - \frac{1}{R_i}(T_i - T_m) - Q + I_g A_w\right)dt + \sigma_1 d\omega_1 \\ dT_m = \frac{1}{R_i C_m}(T_i - T_m)dt + \sigma_2 d\omega_2 \end{cases} \quad (1)$$

The SDE presented in equation (1) is a continuous-time model for heat dynamics. Since the data collection is discrete, equation (1) must be discretized by integrating over the sampling interval [t, t+s), assuming that all the input parameters are constant in an interval. The process is completely described in [18, 19]. The resulting discrete model is presented in equation (2):

$$\begin{cases} {T_i}^{t+1} = \emptyset_{11}\,{T_i}^{t} + \emptyset_{12}\,{T_m}^{t} + \emptyset_{13}\,{T_a}^{t} + \emptyset_{14}\,{I_g}^{t} + \emptyset_{15} Q^t + v_1(t)^t \\ {T_m}^{t+1} = \emptyset_{21}\,{T_i}^{t} + \emptyset_{22}\,{T_m}^{t} + \emptyset_{23}\,{T_a}^{t} + \emptyset_{24}\,{I_g}^{t} + \emptyset_{25} Q^t + v_2(t)^t \end{cases} \quad (2)$$

We are interested to characterize the thermal dynamics after pre-cooling events when the AC is turned off. Hence, the term Q is removed from the model because it is equal to zero during the period of interest. Since there is no measurement of thermal mass temperature, and only the temporal variation of indoor temperature is measured, the term T_m must be omitted from equation (2). To do so, by adjusting the time and developing the second relation for $T_m{}^t$, this term is substituted into the first relation and assuming ${T_m}^{t-1} \approx {T_i}^{t-1}$, the temporal evolution of indoor temperature is obtained according to equation (3):

$${T_i}^{t} = \theta_1\,{T_i}^{t-1} + \theta_2\,{T_i}^{t-2} + \theta_3\,{T_a}^{t-1} + \theta_4\,{T_a}^{t-2} + \theta_5\,{I_g}^{t-1} + \theta_6\,{I_g}^{t-2} + v(t)^t \quad (3)$$

In this equation, all the time indices are shifted by one to formulate ${T_i}^{t}$, instead of ${T_i}^{t+1}$. Hence, t-2 has appeared in time indices. This is a second-order autoregressive model that calculates the current indoor air temperature as the output. To study the relation between input and output signals, the transfer function of the model can be obtained using Z-transform, as shown in equation (4) [19]:

$${T_i}^{t} = \frac{(\theta_3\beta + \theta_4\beta^2)\,{T_a}^{t}}{(1 - \theta_1\beta + \theta_2\beta^2)} + \frac{(\theta_5\beta + \theta_6\beta^2)\,{I_g}^{t}}{(1 - \theta_1\beta + \theta_2\beta^2)} \quad (4)$$

in which β is a backshift operator ($\beta\,{T_i}^{t}={T_i}^{t-1}$). Using the roots of the denominator in equation (4), the time constants can be obtained using equation (5) [18]:

$$\tau_j = \frac{s}{\ln|q_j|}\ \forall j \in [1,2] \quad (5)$$

In which s is the sampling time and q_j is the roots of the denominator of the transfer function. The sampling time of the original dataset is 1 hour, but to capture the short-term dynamics, the data is interpolated linearly, and the sampling time is converted to 10 minutes.

1.5 PARAMETER ESTIMATION

The main model that represents the evolution of indoor air temperature is based on equation (3). The coefficients of this model are obtained by least-square fit, using the AccuRate dataset. Then, using the identified model parameters, roots of the denominator of equation (4) are calculated and passed to equation (5) to calculate time constants. SciPy library [23] that is a Python scientific tool for various mathematical operations, including linear algebra, was used to obtain model parameters. The coefficient of determination of the fit for all the zones is around 99%. Moreover, the distribution of error is near zero with negligible standard deviation, for all the zones. This confirms that the coefficients obtained through least-square fit are reliable to describe the dynamics of the system.

1.6 RESULTS AND DISCUSSION

To have an estimation of the thermal behaviour of each case study building, the average of its zones' time constants was calculated and presented in Table 2. The highest and lowest τ_2 belong to M and B, respectively, while the highest and lowest τ_1 belong to M_2 and M, respectively. It highlights that the short response of these buildings is different from their long response, and a building that responds slower in a long period might have a quicker short response. In other words, the rate of heat transfer between the thermal mass and indoor air might not have a direct relationship with the heat transfer rate between indoor and outdoor environments.

Table 2. Time constants averaged across all the zones for each case study.

	B	M	M_2
$\boldsymbol{\tau_1}$ [mm]	17	14	19
$\boldsymbol{\tau_2}$ [h:mm]	3:08	5:56	4:10

Figure 2 illustrates the joint plot of the time constants associated with each zone, with their distributions. Based on this figure and Table 2, in terms of the heat transfer between indoor and outdoor environments, B has the fastest response, with a τ_2 about 3 hours. τ_2 of M is approximately 6 hours which makes it the slowest building. From the magnitude of τ_2, the level of insulation, solar heat gain, and airtightness of the buildings can be interpreted. Since there is no formulation to directly relate these physical properties to τ_2, its relative values can be used to rank buildings. Another conclusion that can be derived from the magnitude of τ_2 is the ratio of exterior surface area to volume of the building. Higher value of this ratio means higher thermal coupling with the ambient, and consequently faster response (lower τ_2).

On the other hand, τ_1 describes how fast the thermal mass of the building releases heat. Because the heat release rate has a direct relationship with thermal mass properties, and thickness [5], τ_1 can be a reliable metric to compare these parameters related to the thermal mass of different buildings. According to the results, the smallest mean value of τ_1 which is 14 minutes belongs to M, and M_2 has the largest mean value which is 19 minutes. Based on this difference, one can conclude that the thickness of thermal mass in M might be less than that of M_2, which has a slower response [5]. Moreover, the percentage of thermal mass distributed on the surface can be higher in M, which leads to faster heat transfer with indoor air. The location of thermal mass significantly affects thermal dynamics [24] as well. The closer the thermal mass to the surface, the faster the heat transfer.

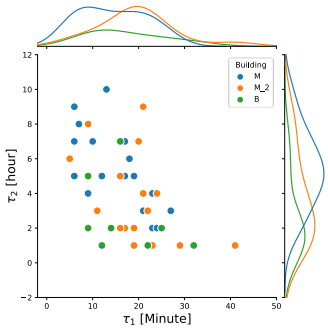

Figure 2. Distribution of time constants for different zones in the three case study buildings.

The conclusions about the thermal dynamics of the three investigated case studies are validated in Figure 3. Building B that has the smallest τ_2, has the fastest response, highest peak, and shortest time in terms of retaining thermal comfort conditions. Conversely, building M, which has the largest τ_2, outperforms the other two buildings in terms of retaining thermal comfort conditions and has the slowest response.

To understand the relationship between the time constants of a zone with its cooling decay profile, the cooling decay profile of each zone is averaged in a month. Figure 4, Figure 5, and Figure 6 illustrate the results for M_2, B, and M, respectively. The analysis is conducted for all the buildings based on the typical meteorological year of Brisbane weather conditions. By visual inspection of the graphs, some interesting relationships can be found. Firstly, the temperature evolution profile of zones with relatively smaller τ_2 peak earlier than those with larger τ_2. For example, in Figure 4, temperature evolution for KitchenMealsF (τ_2 of 1h and 28 min) in January peaks around 7:00 PM while the same graph for Entry (τ_2 of 4h and 27mm) has a peak around 11:00 PM. Moreover, some zones with significantly larger τ_2, such as Pantry, Study, and FF-Powder2, remain thermally comfortable for the next 8 hours if they are pre-cooled to 20°C.

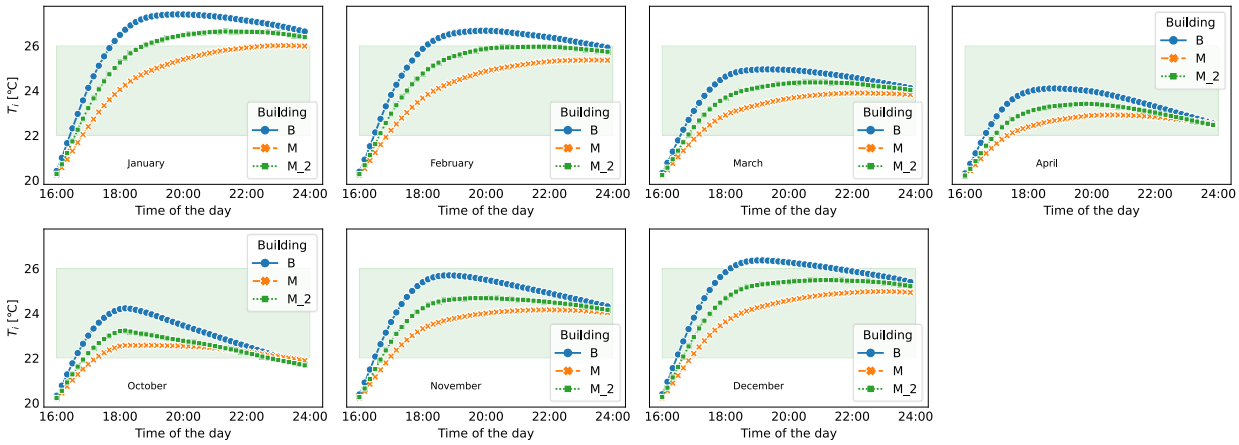

Figure 3. Decay cooling averaged across all the zones in different months.

Since some temperature profiles (e.g., Study in Figure 4) are not even close to the upper limit of thermal comfort, maybe it is not necessary to pre-cool them to 20℃, and higher temperatures at the beginning of the cooling decay might keep them within the thermal comfort range for the rest of the day.

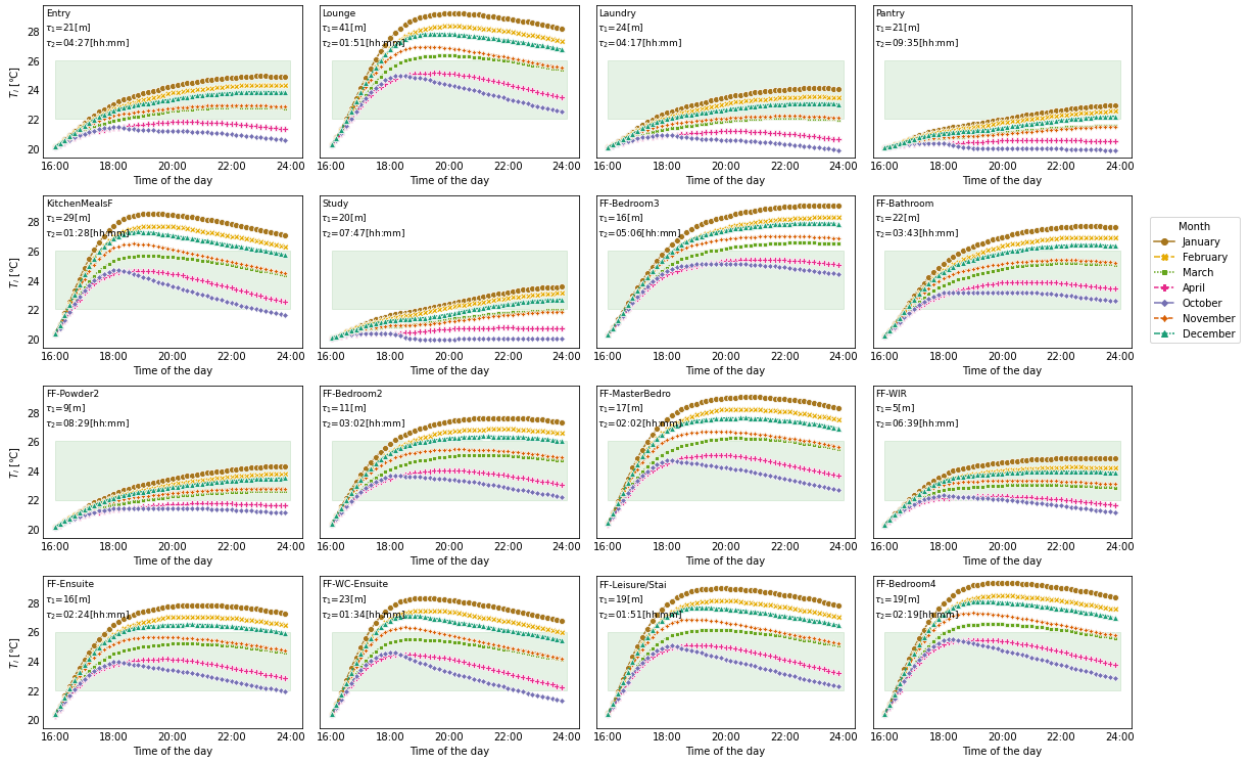

Figure 4. Monthly averaged cooling decay of each zone of M_2, after pre-cooling to 20℃. The green box is the thermal comfort range.

Figure 5 and Figure 6 illustrate cooling decay profiles for buildings B and M, respectively. The same relationships between time constants and cooling decay profile can be observed in these two figures as well. Some zones of M have almost equal τ_2, but different τ_1. For example, FF-Ensuite and Entry have very close values of τ_2, but τ_1 of Entry is about 3 times larger. Consequently, the temperature profile of Entry does not cross 24℃ before midnight while the temperature of FF-Ensuite violates thermal comfort before 8:00 PM and reaches around 27℃ at 11:00 PM. The same behaviour is reported for Living and FF-WIR1. Considering these relationships between τ_1, τ_2, and cooling decay profile, one can conclude that with equal τ_2(long-term time constant), the zone with larger τ_1(short-term time constant) would be more appropriate for pre-cooling because it retains thermal comfort for longer periods. Further investigation of how τ_1 and τ_2 might be related together, and why some zones, like FF-Bedroom3 in M_2, does not keep the indoor temperature within the thermal comfort range despite its relatively large τ_2 are going to be discussed in future works.

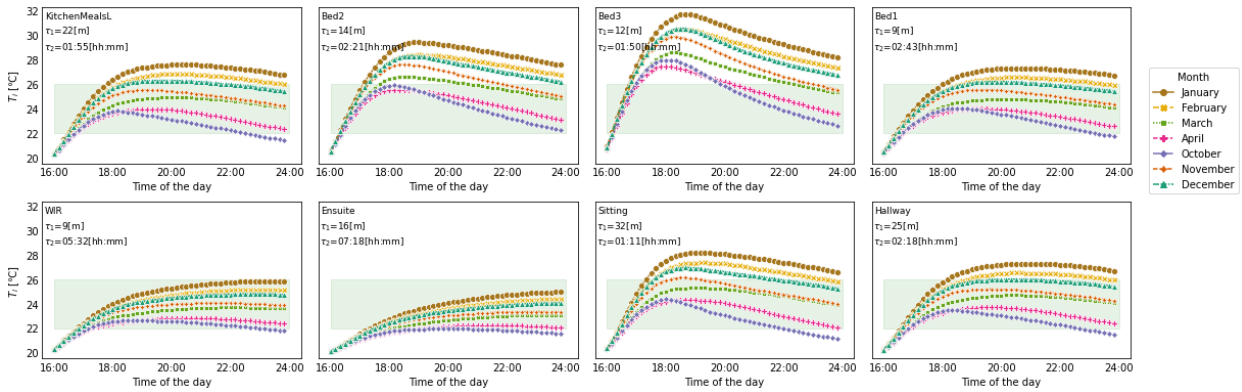

Figure 5. Monthly averaged cooling decay of each zone of B, after pre-cooling to 20℃. The green box is the thermal comfort range.

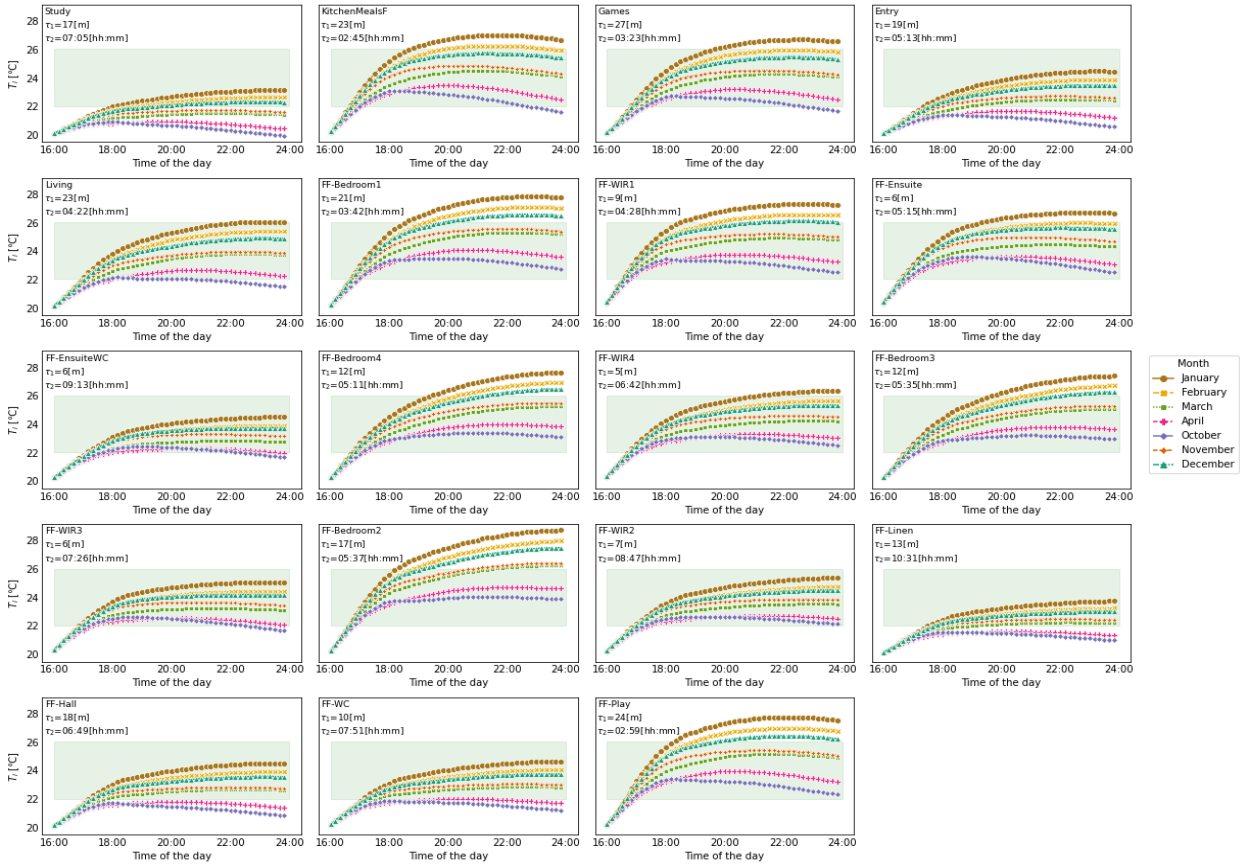

Figure 6. Monthly averaged cooling decay of each zone of M, after pre-cooling to 20℃. The green box is the thermal comfort range.

1.7 CONCLUSIONS

In this paper, the pre-cooling potentials of three multi-zone Australian buildings are investigated by comparing their ability to retain thermal comfort after turning the air conditioner off. The temperature evolution is modelled by simulating the change of indoor air and thermal mass temperatures simultaneously, by deriving an autoregressive model from a second-order linear stochastic differential equation. Then, the transfer function associated with the autoregressive model is constructed and its time constants are obtained. The dataset used in this research is generated by AccuRate, software for rating the energy efficiency of Australian buildings. It is shown that the present model can take solar radiation into account for the calculation of time constants, and is also reliable for cooling applications. Moreover, the simulation of each zone shows that larger time constants delay the peak of indoor temperature significantly. It is also observed that if the long-term time constants of two zones are almost equal, the one with a higher short-term time constant has better performance in terms of retaining thermal comfort conditions. The results highlight that these two time constants that were used for heating applications in previous studies, can be reliable metrics to rank buildings based on their pre-cooling potential, and the ability to maintain the indoor environment cool after each pre-cooling. Whether or not higher time constants lead to more cost savings and peak load reduction associated with pre-cooling can be discussed in future works.

References

[1] Roberts, M. B., 2019, "The value of co-operation: Opportunities for deployment of rooftop photovoltaics on Australian apartment buildings," The University of New South Wales Sydney, Australia.

[2] Simon Heslop, M. R., Baran Yildiz, Anna Bruce, Renate Egan, Iain MacGill, 2019, "Temporal patterns of residential air conditioning consumption in Australia's eastern capital cities," Asia-Pacific Solar Research Conference.

[3] Wood, A. J.; Wollenberg, B. F.; and Sheblé, G. B., 2013, Power generation, operation, and control, John Wiley & Sons.

[4] Braun, J. E., 2003, "Load control using building thermal mass," Journal of Solar Energy Engineering-transactions of The ASME, 125(3), pp. 292-301.

[5] Chen, Y.; Xu, P., et al., 2020, "Experimental investigation of demand response potential of buildings: Combined passive thermal mass and active storage," 280, p. 115956.

[6] Olsthoorn, D.; Haghighat, F., et al., 2017, "Abilities and limitations of thermal mass activation for thermal comfort, peak shifting and shaving: A review," Building and Environment, 118, pp. 113-127.
[7] Turner, W. J.; Roux, J.; and Walker, I. S., 2014, "Reducing residential peak electricity demand with mechanical pre-cooling of building thermal mass."
[8] Wang, J.; Tang, C. Y.; and Song, L., 2020, "Design and analysis of optimal pre-cooling in residential buildings," Energy and Buildings, 216, p. 109951.
[9] Sun, Y.; Wang, S., et al., 2013, "Peak load shifting control using different cold thermal energy storage facilities in commercial buildings: A review," Energy conversion and management, 71, pp. 101-114.
[10] Tabares-Velasco, P. C.; Speake, A., et al., 2019, "A modeling framework for optimization-based control of a residential building thermostat for time-of-use pricing," Applied Energy, 242, pp. 1346-1357.
[11] Ansi/Ashrae, 2013, "Thermal environmental conditions for human occupancy."
[12] Toure, P. M.; Dieye, Y., et al., 2019, "Experimental determination of time lag and decrement factor," Case Studies in Construction Materials, 11, p. e00298.
[13] Arababadi, R.; Elzomor, M.; and Parrish, K., 2017, "Selection of energy efficiency measures to enhance the effectiveness of pre-cooling in residential buildings in hot arid climate," Science and Technology for the Built Environment, 23(5), pp. 858-867.
[14] Rasmussen, C.; Hviid, C. A., et al., 2021, "Estimating Building Airtightness from Data – A Case Study," 246, p. 10004.
[15] Klaassen, C.; House, J. M.; and Center, I. E., 2002, "Demonstration of load shifting and peak load reduction with control of building thermal mass," Teaming for Efficiency: Commercial buildings: technologies, design, performance analysis, and building industry trends, 3, p. 55.
[16] Ali, Q.; Thaheem, M. J., et al., 2020, "The Performance Gap in Energy-Efficient Office Buildings: How the Occupants Can Help?," 13(6), p. 1480.
[17] Rasmussen, C.; Bacher, P., et al., 2020, "Method for scalable and automatised thermal building performance documentation and screening," 13(15), p. 3866.
[18] Palmer Real, J.; Rasmussen, C., et al., 2021, "Characterisation of thermal energy dynamics of residential buildings with scarce data," Energy and Buildings, 230, p. 110530.
[19] Madsen, H.; and Holst, J., 1995, "Estimation of continuous-time models for the heat dynamics of a building," Energy and Buildings, 22(1), pp. 67-79.
[20] Jiménez, M. J.; Madsen, H.; and Andersen, K. K., 2008, "Identification of the main thermal characteristics of building components using MATLAB," Building and Environment, 43(2), pp. 170-180.
[21] Law, A. M., 2018, "Building Evaluation: The Decay Method as an Evaluation Tool for Analysing Thermal Performance," RMIT University.
[22] CSIRO, 2021, "AccuRate: helping designers deliver energy efficient homes," https://www.csiro.au/en/research/technology-space/it/AccuRate.
[23] Virtanen, P.; Gommers, R., et al., 2020, "SciPy 1.0: Fundamental Algorithms for Scientific Computing in Python," Nature Methods, 17, pp. 261-272.
[24] Wijesuriya, S.; Brandt, M.; and Tabares-Velasco, P. C., 2018, "Parametric analysis of a residential building with phase change material (PCM)-enhanced drywall, precooling, and variable electric rates in a hot and dry climate," Applied Energy, 222, pp. 497-514.